Analysis of pulse modulation format in coded BOTDA sensors

Marcelo A. Soto, Gabriele Bolognini*, Fabrizio Di Pasquale

Scuola Superiore Sant'Anna, via G. Moruzzi 1, 56124 Pisa, Italy
**g.bolognini@sssup.it*

Abstract: A theoretical and experimental analysis of the impact of pulse modulation format on Brillouin optical time-domain analysis (BOTDA) sensors using pulse coding techniques has been carried out. Pulse coding with conventional non-return-to-zero (NRZ) modulation format is shown to induce significant distortions in the measured Brillouin gain spectrum (BGS), especially in proximity of abrupt changes in the fiber gain spectra. Such an effect, as confirmed by the theoretical analysis, is due to acoustic wave pre-excitation and non-uniform gain which depends on the bit patterns defined by the different codewords. A successful use of pulse coding techniques then requires to suitably optimize the employed modulation format in order to avoid spurious oscillations causing severe penalties in the attained accuracy. Coding technique with return-to-zero (RZ) modulation format is analyzed under different duty-cycle conditions for a 25 km-long sensing scheme, showing that low duty-cycle values are able to effectively suppress the induced distortions in the BGS and allow for spatially-accurate, high-resolution strain and temperature measurements being able to fully exploit the provided coding gain (~7.2 dB along 25 km distance) with unaltered spatial resolution (1 meter). Although Simplex coding is used in our analysis, the validity of the results is general and can be directly applied to any intensity-modulation coding scheme.

OCIS codes: (060.2370) Fiber optics sensors; (290.5830) Scattering, Brillouin; (120.4825) Optical time domain reflectometry.

References and links

1. A. Minardo, R. Bernini, L. Zeni, L. Thévenaz, and F. Briffod, "A reconstruction technique for long-range stimulated Brillouin scattering distributed fibre-optic sensors: experimental results," Meas. Sci. Technol. **16**(4), 900–908 (2005).
2. S. Diaz, S. F. Mafang, M. Lopez-Amo, and L. Thévenaz, "A High-performance Optical Time-Domain Brillouin Distributed Fiber Sensor," IEEE Sens. J. **8**(7), 1268–1272 (2008).
3. L. Thévenaz, and S. F. Mafang, "Distributed fiber sensing using Brillouin echoes," Proc. SPIE 7004, 19th International Conference on Optical Fibre Sensors (OFS19), 2008, paper 3N.
4. Y. Dong, X. Bao, and W. Li, "12-km distributed fiber sensor based on differential pulse-width pair BOTDA," Proc. SPIE vol. 7503, 20th International Conference on Optical Fiber Sensors (OFS20), 2009, paper 2G.
5. M. D. Jones, "Using Simplex codes to improve OTDR Sensitivity," IEEE Photon. Technol. Lett. **15**(7), 822–824 (1993).
6. M. A. Soto, G. Bolognini, F. Di Pasquale, and L. Thévenaz, "Simplex-coded BOTDA fiber sensor with 1 m spatial resolution over a 50 km range," Opt. Lett. **35**(2), 259–261 (2010).
7. N. Linze, W. Li, and X. Bao, "Signal-to-noise ratio improvement in Brillouin sensing," Proc. of SPIE vol. 7503, 20th International Conference on Optical Fiber Sensors (OFS20), 2009, paper 6F.
8. T. Horiguchi, K. Shimizu, T. Kurashima, M. Tateda, and Y. Koyamada, "Development of a Distributed Sensing Technique Using Brillouin Scattering," J. Lightwave Technol. **13**(7), 1296–1302 (1995).
9. D. Alasia, M. González Herráez, L. Abrardi, S. Martin-López, and L. Thévenaz, "Detrimental effect of modulation instability on distributed optical fiber sensors using stimulated Brillouin scattering," Proc. SPIE 5855, 17th International Conference on Optical Fibre Sensors (OFS17), 2005, pp. 587–590.
10. X. Bao, A. Brown, M. Demerchant, and J. Smith, "Characterization of the Brillouin-loss spectrum of single-mode fibers by use of very short (<10-ns) pulses," Opt. Lett. **24**(8), 510–512 (1999).
11. L. Thévenaz, and J.-C. Beugnot, "General *analytical* model for distributed Brillouin sensors with sub-meter spatial resolution" in 20th International Conference on Optical Fiber Sensors (OFS20), 2009, paper 6A.

#128201 - $15.00 USD Received 10 May 2010; revised 16 Jun 2010; accepted 22 Jun 2010; published 28 Jun 2010

1. Introduction

The technique of Brillouin optical time-domain analysis (BOTDA) allows for implementation of fiber-optic distributed sensors with a high accuracy in strain or temperature detection [1,2], finding a broad variety of applications in structural health monitoring, geo-technical engineering and leakage detection along pipelines. BOTDA has been the subject of intense research activities at an international level, both in industry and academia, leading to BOTDA-based schemes attaining long-range [1,2] as well as sub-meter resolution [3,4].

A recently studied topic has been the application of pulse coding techniques [5] in BOTDA sensors [6,7], providing substantial benefits in the attained signal-to-noise ratio (SNR) and keeping an unaltered spatial resolution. BOTDA systems based on such schemes have shown to be able to reach sensing distances of 50-km with a 1-m spatial resolution [6]. However, when using long coded-pulse sequences to significantly improve the SNR, additional effects need to be taken into account; in particular, the dynamics of the acoustic-wave excitation can then come into play, potentially leading to trace distortions and accuracy impairments. Actually, the acoustic wave might be pre-excited to a different extent within different codewords, thus affecting the Brillouin gain and leading to a highly code-dependent probe signal amplification. It is then necessary to carefully analyze such an effect and its impact on coded-BOTDA sensors.

In this paper, we study the impact of pulse modulation format on coded-BOTDA sensors with 1 meter spatial resolution (10 ns pulse width). Theoretical and experimental results show that, in the absence a careful optimization of the modulation format, different codeword-dependent Brillouin gain levels can be experienced by the probe signal, thus leading to distortions in the Brillouin gain spectrum (BGS) and to spurious oscillations affecting the sensors accuracy. Such detrimental effects have been found to stem from acoustic-wave pre-excitation within codeword bits, as confirmed by the theory, and can be effectively avoided by using an optimized return-to-zero (RZ) modulation format, where sufficiently small duty-cycle values effectively suppress the acoustic-wave pre-excitation to negligible levels. Although our analysis has been carried out considering Simplex coding, its validity is general and can be directly applied to other intensity-modulation coding schemes, such as linear and correlation-based codes, where the acoustic-wave pre-excitation issue is also expected to play a fundamental role.

2. Theoretical background of Simplex-coded BOTDA sensors

Stimulated Brillouin scattering (SBS) is a process in which two counter-propagating optical waves, the so-called pump and probe signals, interact with acoustic phonons along an optical fiber [1,2]. In conventional BOTDA sensors with Brillouin gain configuration, a strong pulsed pump wave at a frequency v_0 is sent in forward direction along the sensing fiber, and interacts with a weak continuous-wave (CW) probe beam that propagates in the backward direction, at a lower frequency $v_0 - \Delta v$. This probe-pump interaction actually produces a periodic perturbation of the refractive index of the fiber, reinforcing the acoustic wave through electrostriction effect and leading to an energy transfer among the optical waves. This gain/depletion process takes place whenever pump and probe signals spatially overlap and the frequency difference between the optical waves is within the local BGS [1]. The frequency at which the maximum Brillouin amplification occurs is called Brillouin frequency shift (BFS) and is linearly dependent on strain and temperature variations. Thus, changes in the BFS measured along the sensing fiber (ΔBFS) can be expressed as a linear combination of both temperature (ΔT) and strain ($\Delta\varepsilon$) variations, as follows [8]

$$\Delta BFS(z) = C_{\nu_B\varepsilon} \cdot \Delta\varepsilon(z) + C_{\nu_B T} \cdot \Delta T(z), \tag{1}$$

where $C_{\nu B\varepsilon}$ = 0.048 MHz/με and $C_{\nu BT}$ = 1.07 MHz/°C are the strain and temperature coefficients for BFS in silica fibers.

In order to obtain the BFS parameter, the frequency difference between the optical waves is swept within the BGS, in a range of typically some few hundreds of MHz; and the spatial

#128201 - $15.00 USD Received 10 May 2010; revised 16 Jun 2010; accepted 22 Jun 2010; published 28 Jun 2010

resolution is determined by the pump pulse duration. Then, the intensity variations of the CW probe signal (ΔI_{CW}) are measured at the near end of the fiber ($z = 0$) as a function of time t and the optical frequency difference ($\Delta\nu$), obtaining [1]

$$\Delta I_{CW}(t,\Delta\nu) = I_{CWL}\exp(-\alpha L)\{G(t,\Delta\nu)-1\}, \quad (2)$$

where I_{CWL} is the input probe intensity at the far end of the fiber ($z = L$), α is the fiber loss coefficient, L is the fiber length, and $G(t, \Delta\nu)$ is the net Brillouin gain defined as [1]

$$G(t,\Delta\nu) = \exp\left[\int_{v_g t/2}^{v_g t/2+\Delta z} g_B(\xi,\Delta\nu)\, Ip(\xi,\Delta\nu)\, d\xi\right], \quad (3)$$

where v_g is the group velocity, Δz is the spatial resolution (which is proportional to the pulse length), $g_B(\xi,\Delta\nu)$ and $I_P(\xi,\Delta\nu)$ are the Brillouin gain coefficient and the pump intensity at a distance ξ. Neglecting pump depletion, the expression for the pump intensity simplifies to $I_{P0}\exp(-\alpha\xi)$, where I_{P0} is the input pump intensity (at $z = 0$).

From Eq. (3) we can observe that the Brillouin gain, and then the SNR of the measurements, depend on both spatial resolution and pump power [6]. So, in order to reach longer sensing distances with a given spatial resolution, the pump power could be increased, enhancing the SNR and increasing the dynamic range of BOTDA traces. However, the maximum pump power is limited by pump depletion [1,2] and modulation instability [9], resulting in the main factor limiting the sensing distance. Actually, when the pump pulse width is of the order or shorter than the acoustic-phonon lifetime (~10 ns), the SBS interaction drastically drops [3,4], leading to an ultimate spatial resolution in conventional BOTDA sensors of ~1 m, reducing then the SNR of the measurements, and limiting the maximum sensing distance. In this case, $g_B(\xi,\Delta\nu)$ in Eq. (3) should broaden since the effective BGS, when using 10-ns pulses, is given by the convolution of the natural BGS (exhibiting a linewidth of ~20-35 MHz) and the pump pulse spectrum, changing the BGS from a Lorentzian-shaped to a more Gaussian-like profile. This is actually well-described by a pseudo-Voigt profile which is simply a linear combination of both Lorentzian and Gaussian profiles with weights c and (1-c) respectively [10]

$$f_{p-V}(\Delta\nu) = G_{\max}\left\{c\frac{\Delta\nu_B^2}{\Delta\nu_B^2+4(\Delta\nu-\nu_B)^2}+(1-c)\exp\left[-4\ln 2\frac{(\Delta\nu-\nu_B)^2}{\Delta\nu_B^2}\right]\right\}, \quad (4)$$

where G_{max} is the maximum Brillouin gain, ν_B is the BFS and $\Delta\nu_B$ is the full-width at half-maximum (FWHM) BGS linewidth. The spectral broadening taking place in BOTDA sensors with pulse duration of the order of the acoustic-photon lifetime, actually increases the *rms* noise of BFS measurements ($\delta\nu_B$) according to [8]

$$\delta\nu_B = \frac{\Delta\nu_B}{\sqrt{2}(SNR)^{1/4}}, \quad (5)$$

leading to a reduction of both temperature and strain resolution.

In order to increase the SNR, and hence to improve both temperature and strain resolution, the use of optical pulse coding techniques has been recently proposed for long-range sensors based on BOTDA, providing an extended dynamic range in the measurements, not affecting the spatial resolution [6]. This technique is based on a linearization of Eqs. (2)-(3), assuming that the intensity contrast of the measured CW probe signal (ΔI_{CW}) depends linearly on the pump intensity, according to

$$\Delta I_{CW}(t,\Delta\nu) \propto \int_{v_g t/2}^{v_g t/2+\Delta z} g_B(\xi,\Delta\nu)\, Ip(\xi,\Delta\nu)\, d\xi. \quad (6)$$

#128201 - $15.00 USD Received 10 May 2010; revised 16 Jun 2010; accepted 22 Jun 2010; published 28 Jun 2010

The linearity is actually one of the fundamental requirements to apply this kind of pulse coding technique, such as Simplex coding [5], which uses a linear decoding processing, based on a linear response of the fiber. Actually, this linear behavior is valid whenever $g_B(\xi,\Delta\nu)$ can be assumed to be the same for every pump pulse within a codeword. However, when using a pump pulse width similar to the acoustic-phonon lifetime, the transient of the acoustic wave has a relevant impact on the amplification process [11]. Thus, when 10-ns Simplex-coded pulses are used in order to obtain 1-m spatial resolution, the Brillouin gain provided by each pump pulse may depend on the presence of a pre-existing acoustic wave that might have been previously generated by preceding pulses within the same codeword, leading to a nonlinear Brillouin amplification process. In order to analyze in detail the Brillouin interaction taking place in this case, the transient of the acoustic wave should be also taken into account. This can be done considering the following three-waves SBS transient model [11]

$$\begin{aligned}\left(\frac{\partial}{\partial z}+\frac{1}{v_g}\frac{\partial}{\partial t}\right)E_P &= i\frac{1}{2}g_2 Q E_S,\\ \left(-\frac{\partial}{\partial z}+\frac{1}{v_g}\frac{\partial}{\partial t}\right)E_S &= -i\frac{1}{2}g_2 Q^* E_P,\\ \left(\frac{\partial}{\partial t}+\Gamma_A\right)Q &= ig_1 E_P E_S^*,\end{aligned} \tag{7}$$

where E_S, E_P and Q are the normalized amplitudes of the probe (CW Stokes beam), pump and acoustic fields; $g_{1,2}$ are the electrostrictive and electro-optic coupling coefficients, respectively; $\Gamma_A = i(\Omega_B^2 - \Omega^2 - i\Omega\Gamma_B)/2\Omega$ is the frequency detuning parameter, where $\Omega_B/2\pi$ and $\Omega/2\pi$ are the Stokes resonance frequency and the pump-probe frequency difference, respectively, at a giver fiber position [11]. The factor Γ_B is the acoustic damping constant, which is related to phonon lifetime τ_A (~10 ns in silica fibers) and the spectral width of the Brillouin gain ($\Delta\nu_B$) by $\Gamma_B = 1/\tau_A = 2\pi\Delta\nu_B$.

In order to provide a general idea of the transient behavior of the acoustic wave and the corresponding Brillouin gain when using Simplex coding with 10-ns pulses, the system of Eq. (7) has been solved for simple coded-pulse sequences, as for instance, for the first codeword of a 3-bit Simplex code (corresponding to the sequence '101') [5]. In Fig. 1, we can observe that the acoustic-wave amplitude rises from the zero level with the first 10-ns pulse, however, during the following 10 ns, corresponding to a bit '0', the acoustic wave does not have enough time to be completely damped, and hence it rises from an upper level when the third bit is sent. This means that the Brillouin gain resulting from the third bit is significantly larger than the one obtained from the first one, as shown Fig. 1b. From Eq. (7) we can notice that the gain of the probe signal is proportional to the product of both pump and acoustic fields (as also shown Fig. 1b) [11], explaining why a meter-scale spatial resolution can still be achieved when using Simplex coding, regardless the slower transient of the acoustic wave.

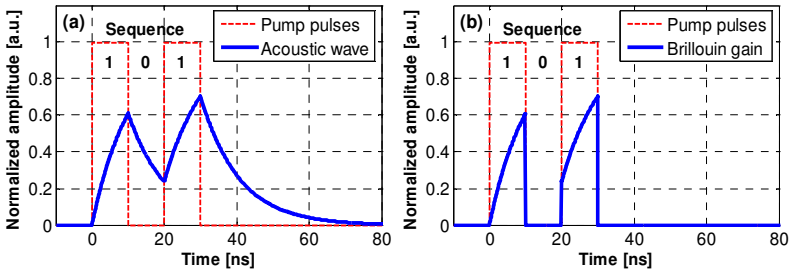

Fig. 1. Transient behavior of conventional Simplex-coded BOTDA sensors. (a) Normalized acoustic-wave amplitude. (b) Normalized Brillouin gain.

#128201 - $15.00 USD Received 10 May 2010; revised 16 Jun 2010; accepted 22 Jun 2010; published 28 Jun 2010

Unfortunately, Simplex coding is based on the linear response of the fiber to the different pump pulses, so that the pre-excitation of the acoustic wave, by previous pump pulses within a codeword (shown in Fig. 1a), can be detrimental for the decoding process. An effective decoding process should take into account the exact transient behavior of the acoustic wave; however, this is not a practical solution since the transients depend on different parameters such as pulse duration, coding length, and frequency separation of the optical waves, among others. A more attractive solution that we are proposing in this paper is the implementation of return-to-zero pulses in BOTDA sensors with meter-scale spatial resolution, providing enough time to the acoustic wave to vanish between two consecutive Simplex-coded pulses, as shown in Fig. 2.

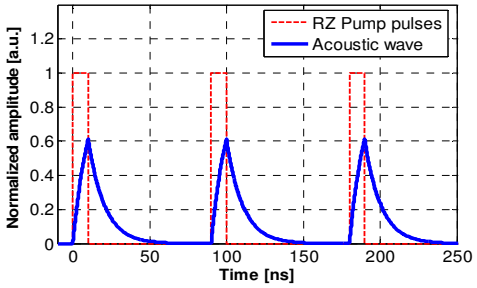

Fig. 2. Normalized acoustic-wave intensity using return-to-zero pulse modulation format.

In the next sections we experimentally and theoretically analyze the negative effects induced by the relatively slow acoustic-wave decay time, when using Simplex-coded BOTDA sensors with conventional 10-ns non-return-to-zero (NRZ) pulses, leading to distortions in the decoded BGS. Then, in order to avoid distortions, the use of return-to-zero Simplex-coded pulses is proposed and analyzed for different duty cycles, allowing for a linear decoding process and undistorted pseudo-Voigt-shaped BGS.

3. Experimental setup

In order to analyze the impact of the pulse modulation format on Simplex-coded BOTDA sensors, the experimental setup shown in Fig. 3 has been used. A distributed-feedback (DFB) laser with ~10 dBm output power operating at 1550 nm has been employed, whose output radiation is then split to generate both pump and probe beams. In the pump branch, an Erbium-doped fiber amplifier (EDFA) has been placed before a Mach-Zehnder modulator (MZM), in order to provide undistorted sequences of Simplex-coded pulses with a high extinction ratio. A waveform generator is connected to the MZM to generate 127-bit Simplex codewords, with individual pulse width of 10 ns, providing an attainable spatial resolution of 1 m. Along the other (probe) branch, the frequency-shifted probe signal is generated by modulating the intensity of the CW light through a MZM controlled by a microwave (RF) generator and a DC bias voltage supplier. By tuning the frequency of the microwave signal, both sidebands generated around the laser carrier frequency are swept around the BFS, so that the distributed BGS along the fiber can be measured. By proper bias adjustment, high suppression of the optical carrier has been obtained. An EDFA followed by a variable optical attenuator (VOA) have been used to properly control the probe power level that is launched into the fiber. A polarization scrambler has also been employed to depolarize the probe signal and hence to reduce polarization-induced fading in the Brillouin gain along the fiber. The sensing fiber is composed of three single-mode fiber spools for an overall distance of ~25 km. Although both sidebands of the probe are sent into the fiber, only the Stokes component is selected at the receiver side by using two optical circulators and a narrowband fiber Bragg grating (FBG, < 0.1 nm bandwidth). A 125-MHz PIN photodiode is connected to an oscilloscope, which is controlled by a computer to perform the measurements and to carry out trace decoding.

#128201 - $15.00 USD Received 10 May 2010; revised 16 Jun 2010; accepted 22 Jun 2010; published 28 Jun 2010

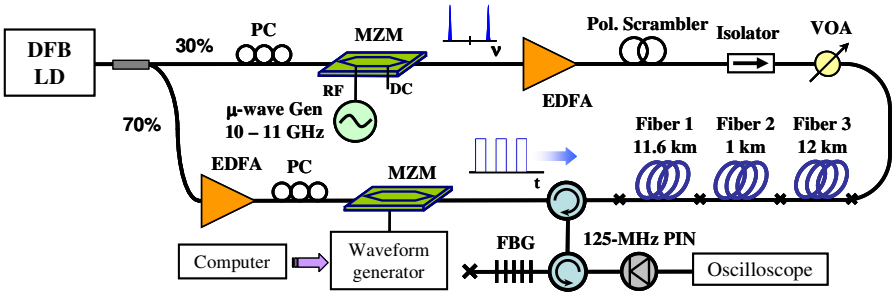

Fig. 3. Experimental setup.

4. Impact of conventional NRZ pulses on BOTDA sensors

Using the experimental setup shown in Fig. 3, we have first analyzed the Brillouin gain characteristics of Simplex-coded BOTDA traces resulting when conventional 10-ns NRZ pulses are used. Figure 4 actually shows six 127-bit Simplex-coded BOTDA traces resulting from six different bit sequences, corresponding to the codewords #1, #8, #32, #64, #96 and #108 of standard S-matrix [5]. It is evident from Fig. 4 that coded traces originated from different codewords give rise to different Brillouin amplification and different normalized intensity levels. Actually, high-intensity coded traces are obtained with codewords containing long bursts of adjacent pulses (bits '1'); considering that the number of pulses (bits '1') is the same in every codeword, it is evident that a nonlinear amplification is taking place in this case. This can be explained by the fact that codewords containing long bursts of consecutive pulses actually allow enough time for the acoustic wave to reach its maximum value, providing a large Brillouin amplification. Thus, for instance, the coded-BOTDA trace obtained with the codeword #64, containing the longest burst of consecutive bits '1' (i.e. 63 adjacent '0's followed by 64 adjacent '1's), exhibits the maximum SBS amplification. This is because, in this case, the acoustic wave is continuously pumped during 640 ns, time which is longer than the one required for the acoustic wave to reach it maximum intensity. Thus, most of the pulses of the codeword strongly interact with the probe wave, providing a large SBS amplification. On the other hand, those codewords containing a uniform distribution of pulses, such as the codeword #1 (i.e., sequence 101010…101), provide weaker Brillouin amplification since the intensity of the acoustic wave does not reach its maximum value within a pulse duration, being continuously interrupted every 10 ns (similarly to the transients reported in Fig. 1). It is possible to clearly observe in Fig. 4 that, depending on the distribution of bits '0' and '1' within codewords, a notably different SBS amplification is obtained when coded pulses with NRZ modulation format are used.

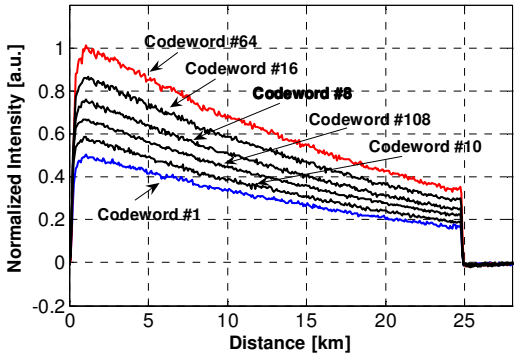

Fig. 4. Coded-BOTDA traces measured with 127-bit Simplex coding based on NRZ pulses.

#128201 - $15.00 USD Received 10 May 2010; revised 16 Jun 2010; accepted 22 Jun 2010; published 28 Jun 2010

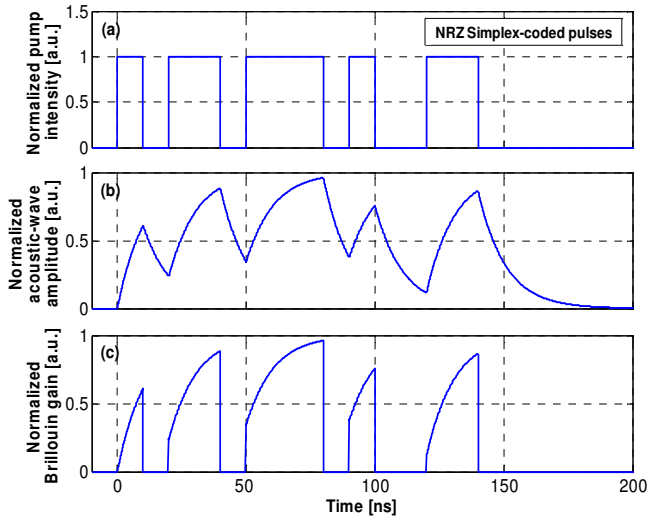

Fig. 5. (a) Simplex-coded sequence based on NRZ pulses, and corresponding (b) normalized acoustic-wave intensity and (c) normalized Brillouin gain.

For a better understanding of this behavior, the system of Eq. (7) has been solved for a particular sequence of NRZ pulses. Figure 5 shows the Simplex-coded pulses, corresponding to the sequence '10110111010011' (Fig. 5a), and the respective normalized amplitude of the acoustic wave (Fig. 5b) as well as the resulting normalized Brillouin gain (Fig. 5c). We can clearly observe that each coded pulse generates a quite different Brillouin gain due to the slow transient of the acoustic wave. It is interesting to notice that even isolated pulses (i.e. pulses which are preceded and followed by a bit '0') provide completely different Brillouin gain depending on their position within the sequence. Thus for instance the bit #10 produces larger gain than the bit #1 due to the pre-existing acoustic wave generated by previous pulses within the codeword. As a consequence, the net Brillouin amplification provided by a specific codeword differs completely from the one obtained by other sequences, even if the number of pulses (number of bits '1') is the same. This leads to a nonlinear SBS amplification, which depends on the bit distribution within the codewords, and produces a detrimental impact on the decoding process, which is based on linear processing techniques.

Considering that the linear decoding process involves summations and subtractions of the acquired coded traces, it is evident that the nonlinear gain shown in Fig. 5 has a maximum impact when large trace differences occur, i.e. at locations where there is an abrupt loss or gain variation. In proximity of such regions, gain imbalance generates spurious oscillations (overshoots and undershoots) during the decoding process at each frequency value, hence distorting the reconstructed BGS.

In order to evaluate the real impact on the decoded BGS, we have changed the temperature of the fiber spool 2 and fiber spool 3, inducing a shift in the BGS of ~17 MHz and ~27 MHz, respectively (with respect to the BGS of the first fiber spool, kept at room temperature). Thus, the BFS along the three fiber spools are ~10.583 GHz, ~10.566 GHz, and ~10.556 GHz, respectively. Actually, Fig. 6 reports the decoded-BOTDA traces corresponding to these three frequencies, where we can clearly see some distortion in the traces due to the presence of both undershoots and overshoots right after the temperature transitions.

#128201 - $15.00 USD Received 10 May 2010; revised 16 Jun 2010; accepted 22 Jun 2010; published 28 Jun 2010

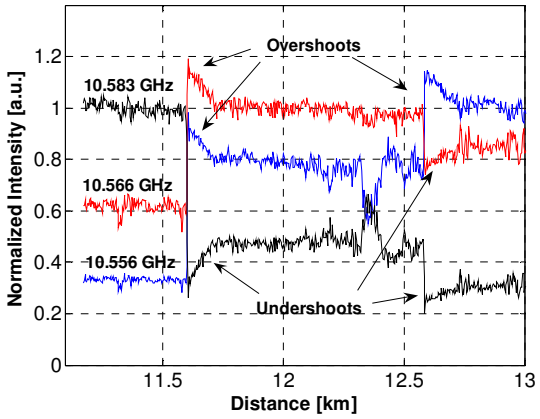

Fig. 6. Coded-BOTDA traces near the temperature transitions, at different frequencies.

This distortion is more evident for frequency values at which a high intensity difference takes place in the CW probe signal between different fibers (i.e. at the peak of the Brillouin gain of every fiber spool), explaining both overshoots and undershoots at those frequencies. However, this effect disappears at frequencies with lower intensity contrast, as shown in Fig. 7, where the decoded BGS is reported as a function of the distance. The origin of this distortion lies in the decoding process, which, assuming a linear fiber response, linearly combines all the coded-BOTDA traces with the same weight when obtaining the decoded BGS. Thus, high-intensity coded traces dominate over lower-intensity traces in the decoding process, inducing an important overlapping of the spatial information along ~127 m (corresponding to the code length), and inducing a distorted BGS over the first meters of both second and third fiber spools. Moreover, the occurring nonlinear SBS gain due to pulse coding has an impact also when no abrupt transition in the detected BGS intensity is found. Actually, considering that the BFS parameter is typically obtained by fitting the measured BGS through a least-mean-square algorithm, we can then figure out how the distortions originated in the decoding process can easily impact on the fitting and induce errors in the obtained BFS parameter. Figure 8a shows both measured and fitted BGS at 11-km distance (over the first fiber, where no abrupt transition occurs in this case), exhibiting a Lorentzian profile with a linewidth of ~35 MHz (similar to the natural Brillouin linewidth), which is not in agreement with the expected broadened pseudo-Voigt profile obtained when using 10-ns pulses [10]. This phenomena can be explained by the same reason of the previously reported distortions, that is the decoded BGS which is obtained by a linear decoding process and is mainly dominated by high-intensity coded traces originating from the strong acoustic wave, thus inducing then a decoded BGS with Lorentzian profile which is similar to the natural BGS profile (instead of the pseudo-Voigt profile expected at such short pulse width [10]).

Taking into account that the accuracy in BFS measurements depends on the Brillouin gain linewidth (see Eq. (5)), this feature may appear as an advantage of the use of NRZ Simplex-coded pulses, with respect to the use of single pulses, which actually provides broadened BGS. However, the distortions induced in the BGS when using NRZ pulses make such modulation format not usable in practice, as already shown in Fig. 7. A clear example of such distortions in the decoded BGS is shown in Figs. 8b and 8c, which show the presence of a dip near the frequencies corresponding to the BGS of the previous fiber. This is produced by a high-intensity contrast in the measured coded-BOTDA traces in that spectral region, and leads to a non-negligible error in the spectrum reconstruction as well as in the fitting process, which exhibits a shift of the obtained BFS equal to ~4-6 MHz with respect to the frequency corresponding to the measured peak value of distorted Brillouin gain.

#128201 - $15.00 USD Received 10 May 2010; revised 16 Jun 2010; accepted 22 Jun 2010; published 28 Jun 2010

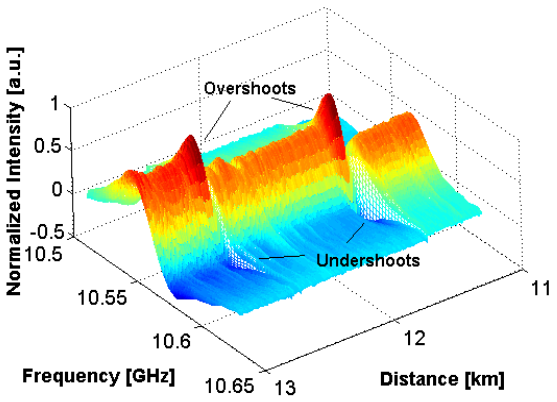

Fig. 7. Decoded BGS as a function of the distance, near the temperature transitions, when using 127-bit Simplex coding with NRZ pulses.

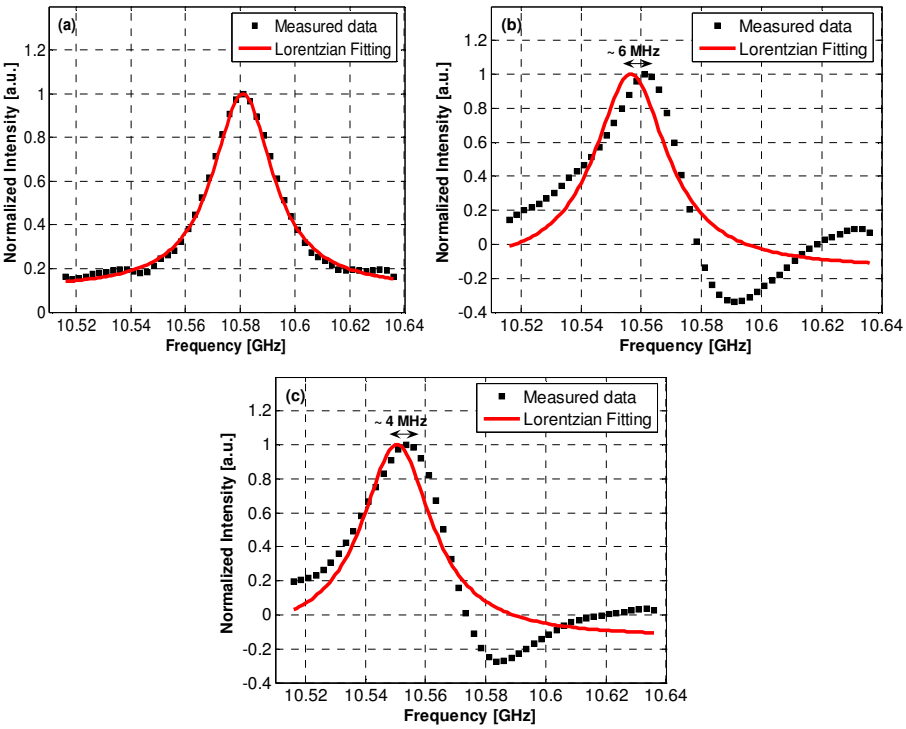

Fig. 8. Measured (decoded) and fitted BGS at a distance of (a) 11 km, (b) ~11.6 km, and (c) ~12.6 km, when using Simplex coding with NRZ pulses.

On the other hand, it is interesting to note that when the BFS abruptly changes on a wider spectral scale, the impact of the occurring spectral BGS distortions on the fitting process, leading to BFS parameter, is reduced to a smaller extent. Figure 9 actually reports this situation, when a change of ~100 MHz is induced in the BFS. We can clearly observe the presence of both an overshot and an undershoot in the decoded spectrum as a function of the distance (see Fig. 9a). Analyzing the local BGS at ~11.6 km (at the beginning of the second fiber), a dip in the decoded spectrum can be observed at a frequency separation of ~100 MHz from the corresponding BFS (resulting from the BGS in the previous fiber); this distortion is found to have a minimum impact on the Lorentzian fitting, which actually gives the proper BFS (see Fig. 9b).

#128201 - $15.00 USD Received 10 May 2010; revised 16 Jun 2010; accepted 22 Jun 2010; published 28 Jun 2010

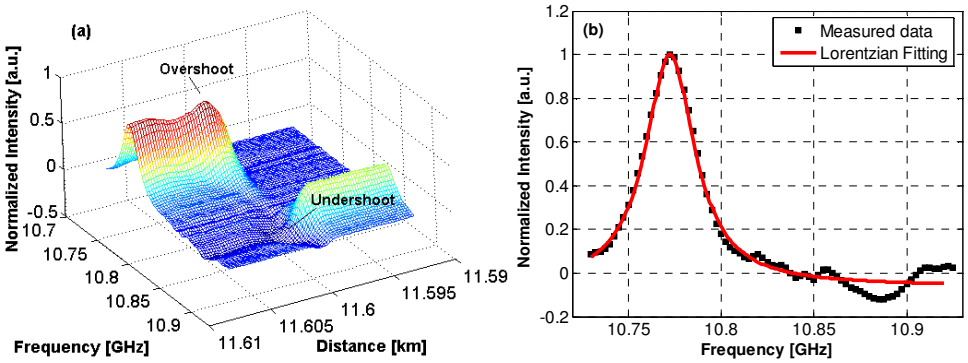

Fig. 9. (a) Measured BGS vs distance. (b) Measured and fitted BGS at ~11.6-km distance.

5. Impact of RZ pulses on BOTDA sensors

In order to avoid the distortions observed in the previous section, the use of RZ pulses provides an attractive pulse modulation solution that allows for a uniform SBS amplification over the different Simplex-coded traces. Thus, every bit of the Simplex codewords can be replaced by the use of an RZ pulse as illustrated in Fig. 10; while the pulse width determines the spatial resolution, a following 'zero level' gives time to the acoustic wave to be damped. If a spatial resolution of 1 m is required, then the pulse width should be 10 ns, while the full bit slot, determining the duty cycle, can be properly chosen to provide a uniform SBS amplification over all the Simplex-coded BOTDA traces.

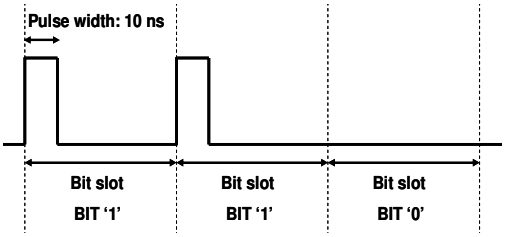

Fig. 10. Simplex coding based on RZ pulses.

Since coded-BOTDA traces obtained with codewords #1 and #64 are the ones with lower and higher SBS amplification respectively (as reported in Fig. 4), we can then analyze the impact of RZ pulses over these two traces only, since all the other coded traces will exhibit intensity values in between those two codewords. Figures 11a-11c report the BOTDA-coded traces obtained with both codewords #1 and #64 when using NRZ Simplex-coded pulses (equivalent to the traces in Fig. 4) and RZ Simplex-coded pulses with duty cycles of 25% and 16.7%, respectively. It is evident that when using RZ format the intensity difference between the two coded traces is reduced depending on the duty cycle.

#128201 - $15.00 USD Received 10 May 2010; revised 16 Jun 2010; accepted 22 Jun 2010; published 28 Jun 2010

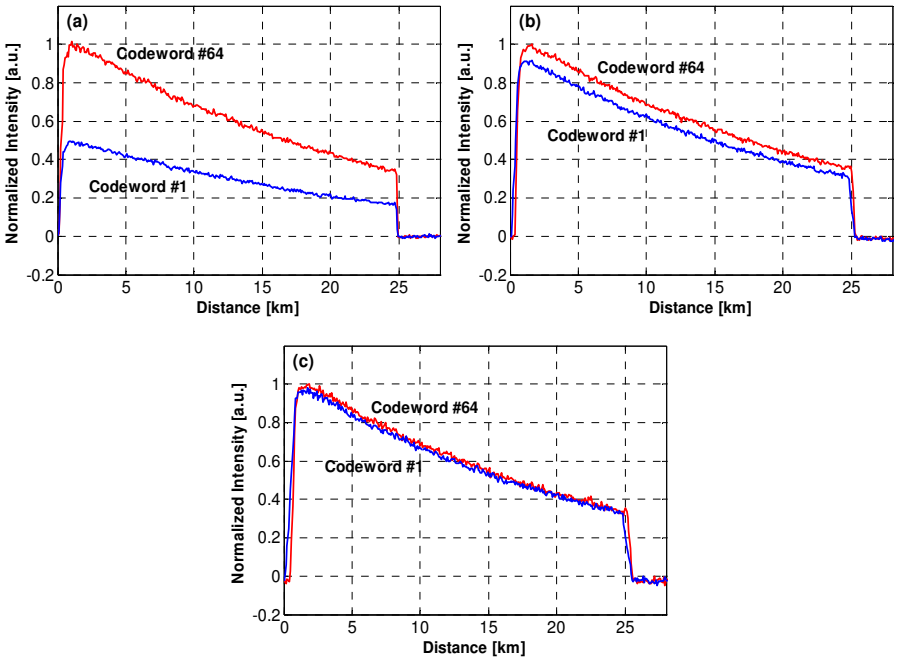

Fig. 11. Normalized intensity for coded-BOTDA traces obtained with codewords #1 and #64. (a) Using NRZ pulses. (b) Using RZ pulses with 25% duty-cycle. (c) Using RZ pulses with 16.7% duty-cycle.

The effectiveness in the different implementations of RZ pulses in Simplex coding is evaluated and compared by calculating the maximum intensity difference among Simplex-coded traces (the extreme intensity values are found for traces corresponding to codewords #1 and #64), giving

$$Difference(\%) = \frac{\mathrm{Max}(Coded\ trace\ 64) - \mathrm{Max}(Coded\ trace\ 1)}{\mathrm{Max}(Coded\ trace\ 64)} x100\,. \qquad (8)$$

Figure 12 actually shows such a relative intensity difference as a function of the bit slot, where 10 ns corresponds to the NRZ format and larger bit slots correspond to RZ format with different duty cycle values (while keeping 10-ns pulse-width to ensure 1-m spatial resolution).

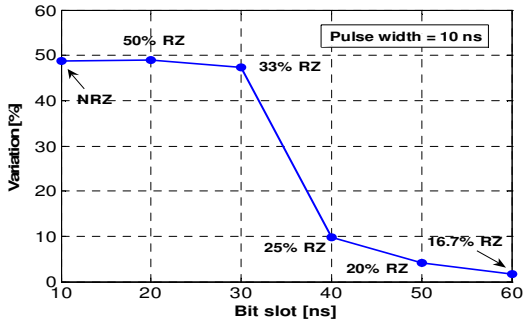

Fig. 12. Relative intensity difference as a function of the bit slot.

We can observe that, when using a RZ format with a 'zero level' which is longer than about 30 ns (bit slot ≥ 40 ns), then both coded traces exhibit a similar SBS amplification; thus, leading to an expected reduction of the distortion in the respective decoded BOTDA traces. This value is in agreement with the theoretical prediction of complete acoustic-wave damping,

#128201 - $15.00 USD Received 10 May 2010; revised 16 Jun 2010; accepted 22 Jun 2010; published 28 Jun 2010

since 30 ns corresponds to approximately $3\tau_A$, where τ_A is the acoustic decay time in silica fibers (~10 ns). Actually, the intensity difference between the two coded traces is reduced from ~50% with NRZ pulses down to ~1.6% when using RZ pulses with a duty cycle of 16.7% (bit slot of 60 ns) as shown in Fig. 12. This duty cycle actually provides a uniform amplification for all Simplex-coded BOTDA traces, as shown in Fig. 13, reporting the behavior with RZ pulses of the traces corresponding to the same codewords as from Fig. 4. This behavior can also be theoretically verified when solving the three-coupled equations describing the transient of the SBS interaction. As we can see in Fig. 14 (where the same sequence reported in Fig. 5 is analyzed), a duty cycle of 16.7% provides enough time to the acoustic wave to be damped after a 10-ns pulse and before the next pulse occurs (see Fig. 14b). Thus, the acoustic wave is uniformly excited during each pump pulse within a codeword, thus providing a uniform Brillouin amplification, as shown Fig. 14c. This behavior demonstrates that the use of Simplex coding using RZ pulses effectively suppresses the interaction of pump pulses with the pre-existing acoustic wave, so that each pump pulse within a codeword provides the same Brillouin gain, which then turns out to be totally independent of the bit distribution.

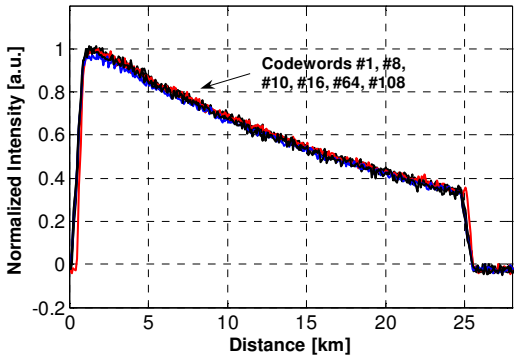

Fig. 13. Coded-BOTDA traces measured with 127-bit Simplex coding base on RZ pulses with 16.7% duty cycle.

When the BGS shown in Fig. 7 is measured using RZ Simplex-coded pulses with 16.7% duty cycle, the decoded BGS along the fiber does not exhibit any distortion, as shown in the spectrum of Fig. 15. Actually, the linear amplification provided by each pump pulse does not induce any distortion in the linear decoding process. Figure 16 reports the local BGS measured at a distance of 11 km, ~11.6 km and ~12.6 km (equivalent to the spectra shown in Fig. 8), exhibiting a proper pseudo-Voigt profile as evident from the fitting curve of Fig. 16. The decoded BGS has an enlarged linewidth of ~100 MHz, as expected when using conventional single-pulse BOTDA with 10-ns pulses [10] and confirming acoustic-wave pre-excitation suppression.

#128201 - $15.00 USD Received 10 May 2010; revised 16 Jun 2010; accepted 22 Jun 2010; published 28 Jun 2010

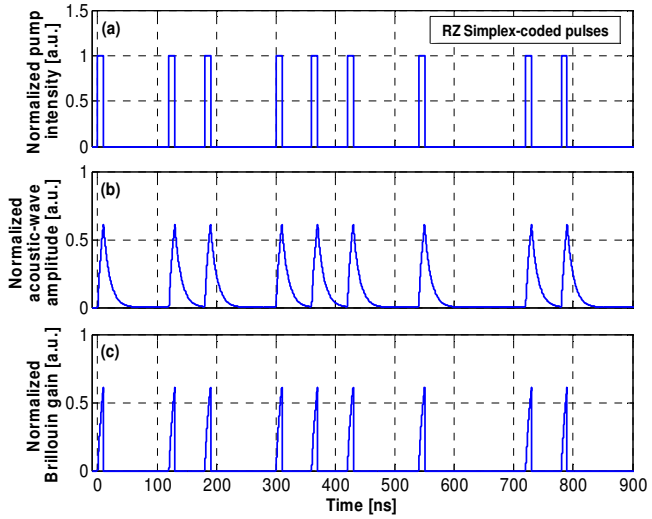

Fig. 14. (a) Simplex-coded sequence based on RZ pulses with 16.7% duty cycle, and corresponding (b) normalized acoustic-wave intensity and (c) normalized Brillouin gain.

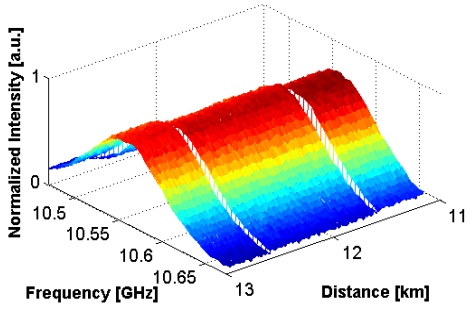

Fig. 15. Decoded BGS as a function of the distance, near the temperature transitions, when using 127-bit Simplex coding with RZ pulses (16.7% duty cycle).

It is important to point out that the BGS broadening, taking place when using short pulses, slightly reduces the accuracy of the BFS measurements (according to Eq. (5)), thus affecting the final temperature and strain resolution of both coded and conventional BOTDA sensors at meter-scale and shorter spatial resolution. However, in our proposed system, the measurement SNR is enhanced thanks to the use of RZ Simplex-coded pulses, thus leading to an overall enhanced performance without distortion. Figure 17 actually shows a comparison of the BOTDA traces (measured at the peak BGS frequency of the third fiber spool, ~10.556 GHz) obtained with both 127-bit Simplex coding using RZ pulses with 16.7% duty cycle and the conventional single-pulsed BOTDA. The noise reduction effect provided by coding techniques can be clearly appreciate from Fig. 17, leading to an experimental SNR improvement of ~7.2 dB, in agreement with the theoretical expected value (~7.5 dB) in case of 127-bit code length.

#128201 - $15.00 USD Received 10 May 2010; revised 16 Jun 2010; accepted 22 Jun 2010; published 28 Jun 2010

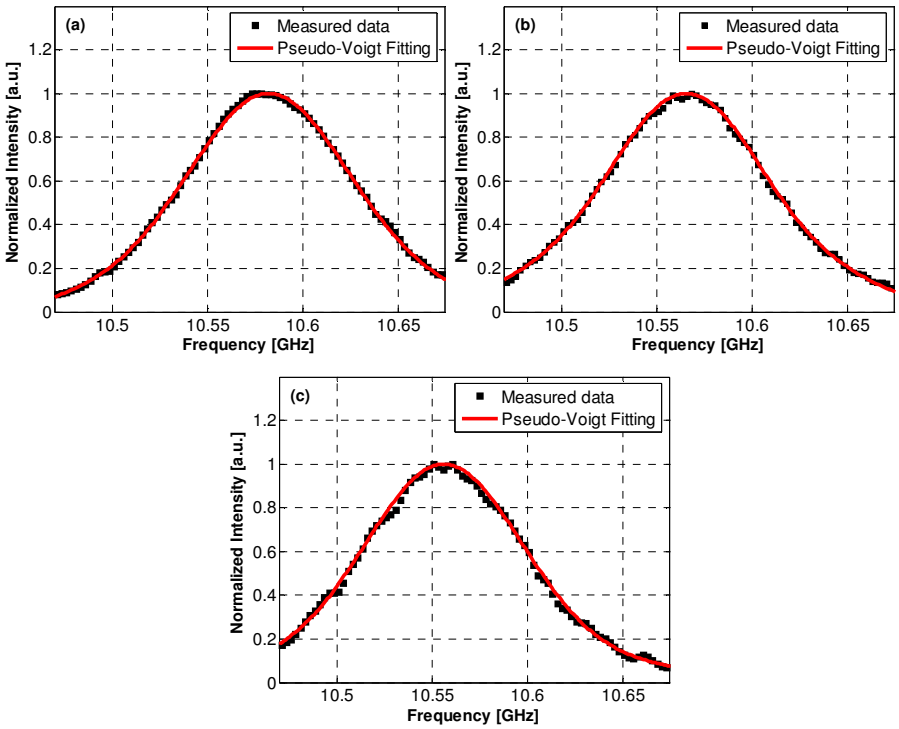

Fig. 16. Measurement and fitting of BGS at a distance of (a) 11 km, (b) ~11.6 km, and (c) ~12.6 km, when using Simplex coding with RZ pulses (16.7% duty cycle).

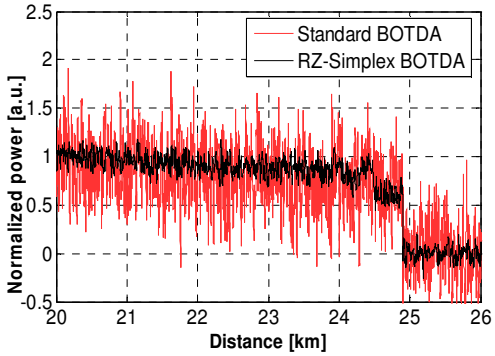

Fig. 17. BOTDA traces at ~10.556 GHz (peak frequency of the third fiber spool) obtained with both 127-bit simplex coding, using RZ pulses with 16.7% duty cycle, and conventional single-pulsed BOTDA

The BFS obtained when using Simplex-coded pulses with RZ modulation format (16.7% duty cycle) is shown in Fig. 18 as a function of the distance (in the neighboring region of the temperature transitions), where we can observe that an unaltered spatial resolution of 1 m is attained with the use of RZ pulses.

#128201 - $15.00 USD Received 10 May 2010; revised 16 Jun 2010; accepted 22 Jun 2010; published 28 Jun 2010

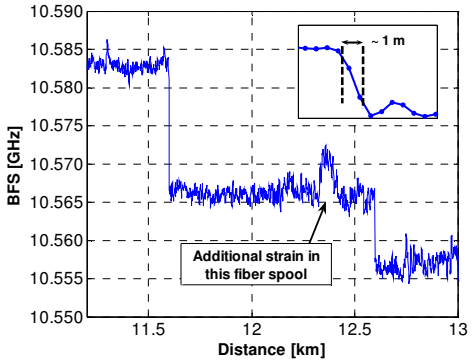

Fig. 18. BFS around temperature transitions using 127-bit Simplex coding with RZ pulses. Inset, achieved temperature resolution.

6. Conclusions

In conclusion, we experimentally and theoretically analyzed the impact of the pump modulation format on coded-BOTDA sensors. A detrimental effect, involving acoustic-wave pre-excitation within coded-BOTDA traces, and leading to severe distortion of the decoded BGS near BFS transition regions, has been identified and analyzed when using conventional NRZ modulation format. The analysis points out that conventional NRZ coded pulses cause severe penalties in the sensing performance (up to 6 MHz inaccuracy in the BFS in our case) and may severely impact the possibility of using pulse coding techniques in BOTDA sensors. In order to suppress such penalties, the use of low duty-cycle RZ pulses has been proposed for BOTDA sensors with meter-scale and shorter spatial resolution. Thus, careful optimization of the pulse modulation format allows for a full exploitation of coding gain, offering an experimental SNR enhancement of ~7.2 dB over 25-km distance when using 1-m spatial resolution.

#128201 - $15.00 USD Received 10 May 2010; revised 16 Jun 2010; accepted 22 Jun 2010; published 28 Jun 2010